maximum deformations at this axis. A high-precision measuring system recorded these deformations: stresses in the reinforcing steel in the pier heads (strain gauges installed when building the piers), the inclination of superstructure (inclination sensor) and the deformation of the bridge joint in longitudinal direction (distance sensors). In addition, geodetic measurements were taken to record the deflections of the superstructure.

**Fig. 10**—Freight trains on the Scherkondetalbrücke

From the analysis of the measured data, which required complex data preparation, it was possible to identify various influencing factors. The results include influence lines showing the curvature of the pier heads, the rotation of the superstructure and the deflection of the superstructure as a function of the position of the trains.

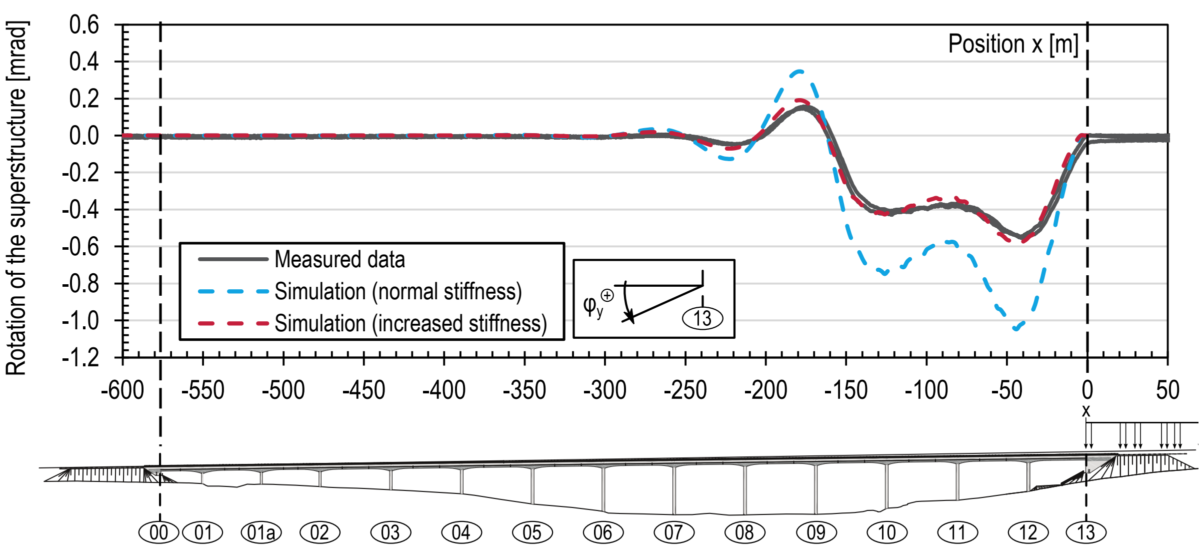


**Fig. 11**—Influence lines for the measured and calculated rotation ($\varphi_y$) of the superstructure at axis 13

Fig. 11 shows the influence lines for the rotation of the superstructure at axis 13 ($\varphi_y$) determined from the measured data and from a numerical model. This rotation is an integral measure for the global deformation characteristic of the semi-integral bridge and allows a good evaluation of the bearing behaviour. Because the bridge behaved more stiffly than expected in the preliminary design calculations, the stiffness of the superstructure in the model was increased by a factor of 1.8. The results of the numerical simulations with the higher stiffness agree very well with the experimental results. Not only had the rotation of the superstructure agreed very well between measuring and calculation, also the comparison between the measured and calculated data of the curvature of the pear heads and the deflection of the superstructure were delivered good results. The assumption of a greater stiffness of the superstructure is justified because the nonballasted track participates in the load transfer of the applied vertical loads.

The test and the way it was performed provided insights into the load-bearing behaviour of Germany's first semi-integral concrete railway bridge and added to the knowledge about this construction method for future railway bridge construction[27]. The system calibration test took place in the serviceability limit state. Therefore, the test does not provide direct information about the ultimate limit state. Nevertheless, the desired goal of a system calibration could be reached with this kind of test and the way of measuring. For future load tests, it could be learned that the measured rotation of the superstructure and the deflection of the superstructure is a good indicator for the global structural deformation behaviour.

## Saale-Elster-Valley bridge (railway bridge)

The Saale-Elster-Valley bridge is also located on the new high-speed railway line between Erfurt and Leipzig/Halle. With a total length of 8,577 m (9,380 yd) the bridge is the longest railway bridge in Germany and is special because the track and the bridge split up and continue as two separate structures. Fig. 12 gives an overview of the bridge and Fig. 13 gives a closer look of the construction itself.

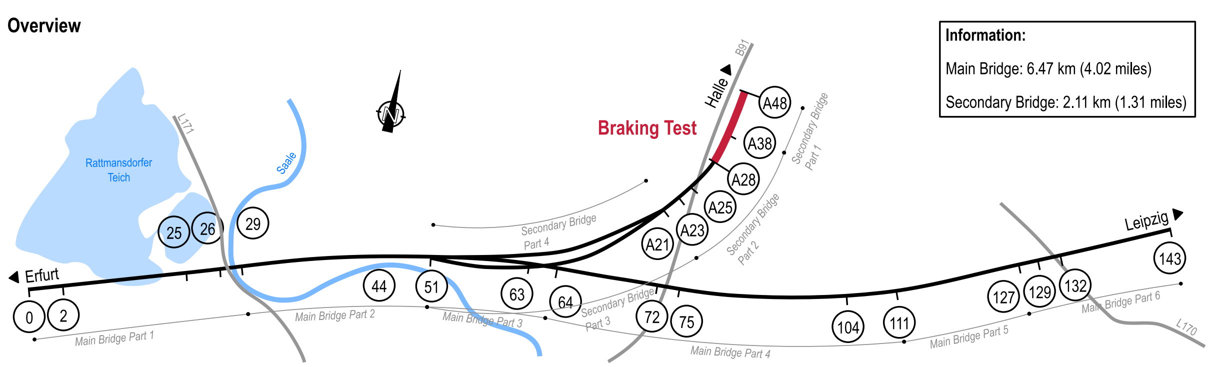


**Fig. 12** —Overview of the whole Saale-Elster-Valley bridge

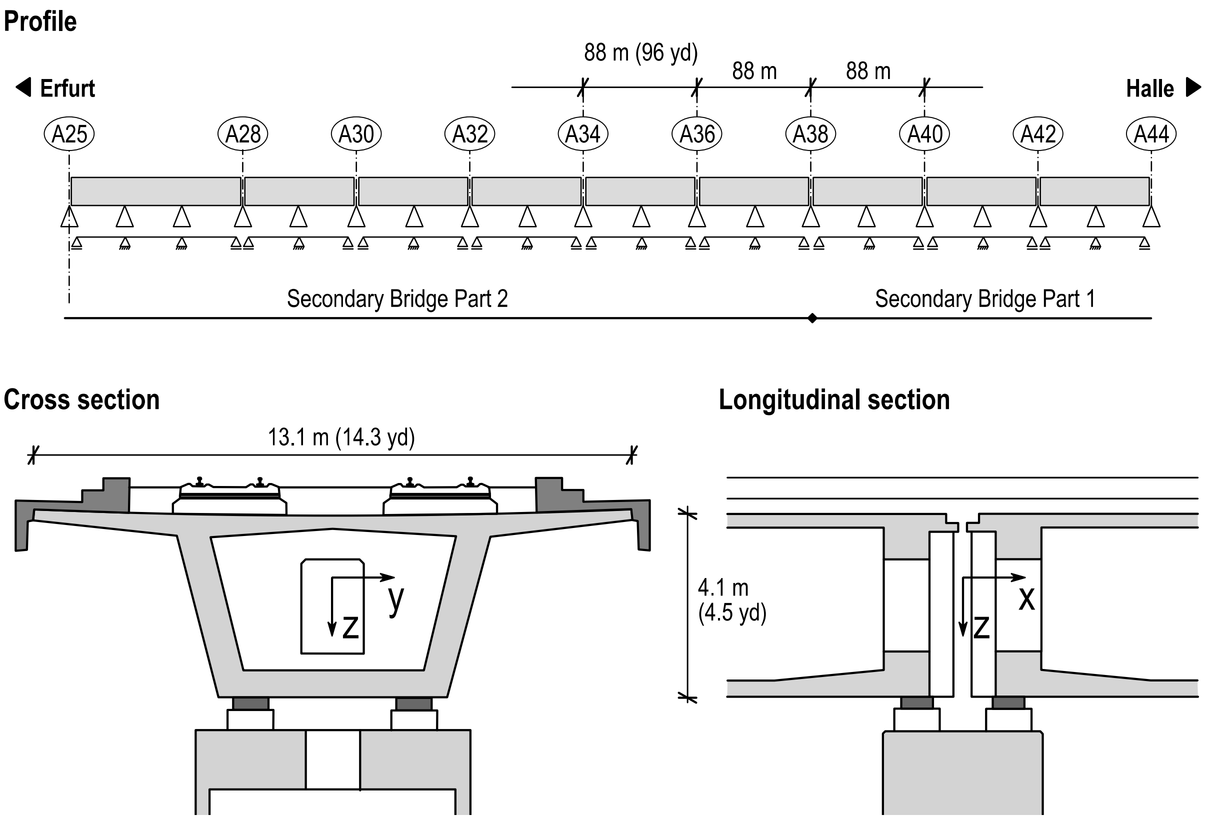


**Fig. 13** —Profile of a part of the secondary bridge, cross section and longitudinal section

Generally the bridge's pre-stressed concrete superstructure is continuous over two spans, with only few exceptions (for example a tied arch bridge around axis 64 where the split up tracks cross). The middle pier of the two-span beams is built as a fixed point.

To verify the assumptions made in the design of the bridge, braking tests were performed between axis A28 to A48[30,31]. These test were diagnostic load test according to table 1. The main goal of the braking tests was to gain information about the actual stiffness of the piers and about the global load-bearing behaviour. The stiffness of the piers was a doubtful size during the design process but it has a main influence on the overall deformation behaviour. Because the stiffness is defined as the quotient of force and displacement, it was necessary to measure the (horizontal) displacement of the piers and the (horizontal) force that is transferred by the piers. The displacement of the piers was measured geodetically, the stresses in the rail were measured with strain gauges on the rails, the deformation of the bridge joints in longitudinal direction with distance sensors and the bearing displacement at the fixed points was monitored with longitudinal displacement transducers. Two heavy loaded freight trains with a length of 80 m (87.5 yd) each and a total weight of 488 t (538 US) per train were used for the braking tests. With slow train passages (maximum speed of 20 km/h (12.4 mph) the numerical model was calibrated and the measuring systems could be checked for plausibility.


**Fig. 14** —Manual signaling to start the braking process with a flag

The evaluation of the braking test showed that the calculated dynamic stiffness of the piers is about 3 to 6 times higher than the static ones from the soil expertise. With these experimentally determined values for the pier stiffness the numerical model was updated. The numerical model contains the part of the secondary bridge between axis A23 and A48. Both, the superstructure and the rails are designed as beam-elements and the piers are either modelled as fixed bearings (fixed points) or as floating bearings (piers at the bridge joints). The results of the comparison between the test and the numerical simulation are presented in Fig. 15. Both results are compared by showing the occurring forces in the rails and the displacements of the bridge joints at the time of braking as a function of the bridge's length.

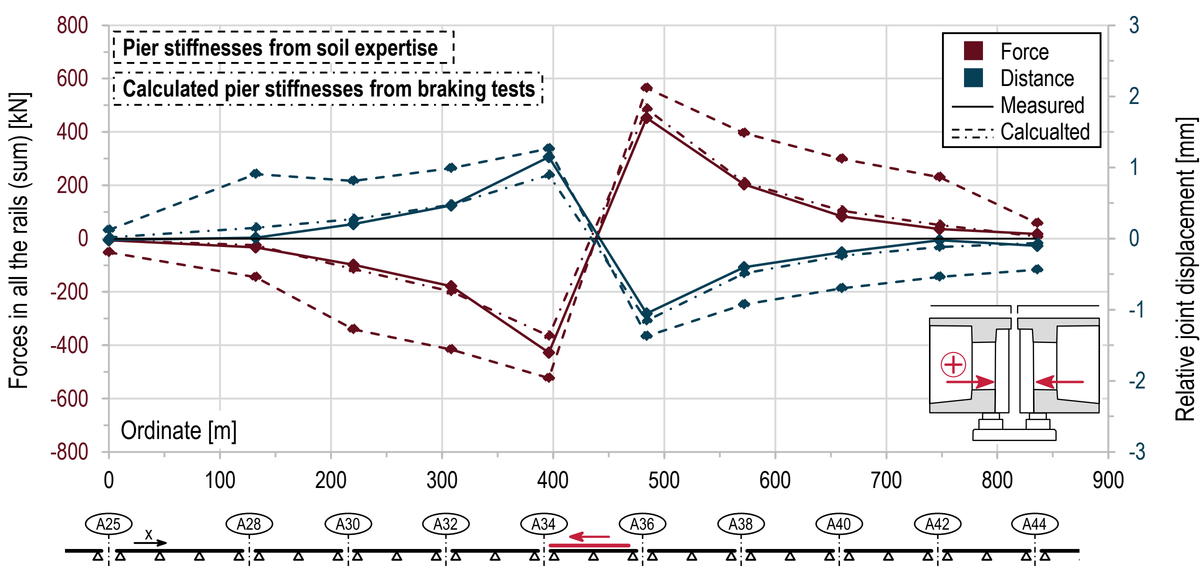


**Fig. 15** —Results of the braking test and numerical calculation before and after calibration of the model

Fig. 15 compares the relative joint displacement measured during the test with the results of the numerical simulation without and with updated values for the pier stiffness. The model prior to the calibration contained the (static) stiffnesses from the soil expertise which were much lower (1/6 to 1/3) than the calculated (dynamic) stiffnesses from the braking tests. The displacement calculated with the calibrated model fits the measured ones very well. In addition, the effective load-bearing length of the bridge can be seen from the evaluation and is is about 350 m (383 yd) in each direction (700 m (766 yd) in total) from the braking position.

With the performed braking test on the Saale-Elster-Valley bridge, the open questions concerning the real stiffness of the piers and global load-bearing behaviour could be answered. The load test successfully supported the numerical simulations for the determination of the load bearing behaviour and demonstrates the potential of experimental assistance in design.

## Measurements at the coupling joints of a road bridge

In a 130 m (142 yd) prestressed concrete road bridge the fatigue check for the tendons at the coupling joints could not be satisfied. Therefore, a diagnostic load test (table 1) was performed, as recommended in the guideline Nachrechnungsrichtlinie[20]. They consisted of long-term measurements to obtain information on the temperature behaviour, and short-term measurements which included a load test.

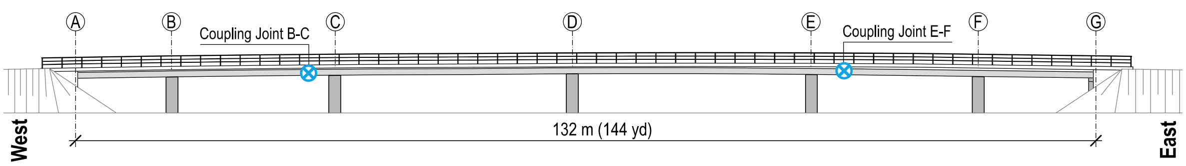


**Fig. 16** —Profile of the bridge, showing the coupling joints

The bridge has two coupling joints, where all tendons running in the longitudinal direction are coupled. Fig. 16 shows the bridge with its seven axes and two coupling joints. The coupling joints are located in the spans between axes B and C, and axes E and F.

The aim of the performed tests was to obtain strain measurements at the – possibly cracked – coupling joints in order to compare them with the measurements taken at various reference measurement locations with uncracked concrete. Such a comparison yields information about the condition of the coupling joints and indicates whether critical cracks exist at the joints. Therefore, the results measured on the coupling joints are compared to measurements on a (uncracked) reference point which is located on a position were similar bending moments to the ones in the coupling joints occur when the trucks are passing.

Strain measurements of the superstructures concrete in the longitudinal direction of the bridge were taken by distance sensors as seen in Fig. 17. The sensors were located in different sections of the bridge as seen in Fig. 19. Several sensors were installed at the two coupling joints and the various reference measurement points. Furthermore, laser measurements of the deflection of the span between axes B and C were performed. The lasers were located on the ground underneath the bridge facing upwards to the superstructure and measuring the deflections of the superstructure as the trucks were passing.

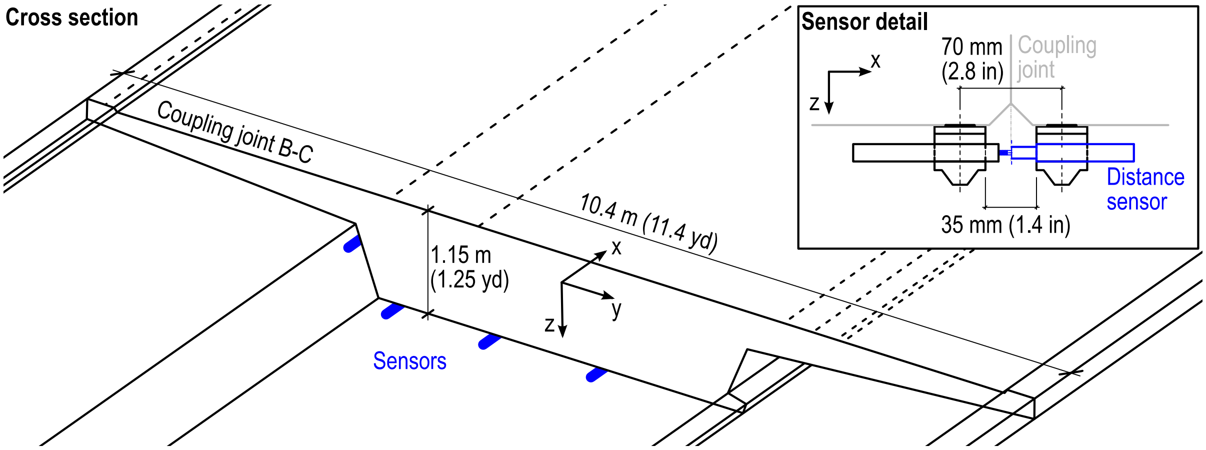


**Fig. 17** —Cross section of coupling joint B-C with sensors and a detail of the application of the sensors

In the performed tests, two 26 t (26.7 US) trucks drove over the bridge one after the other or simultaneously on parallel lanes. The trucks also stopped at specific positions that had been determined beforehand from a numerical model. The stopping positions were chosen to maximise the relevant actions that were to be measured.


**Fig. 18** —Two trucks driving over the bridge simultaneously

The measurement results of the performed test provide insight into the state of the coupling joints. The strains measured at the two coupling joints were much higher than those measured at reference point 2 where the bending moment is similar to that at the coupling joints. Fig. 19 shows a comparison of the results.

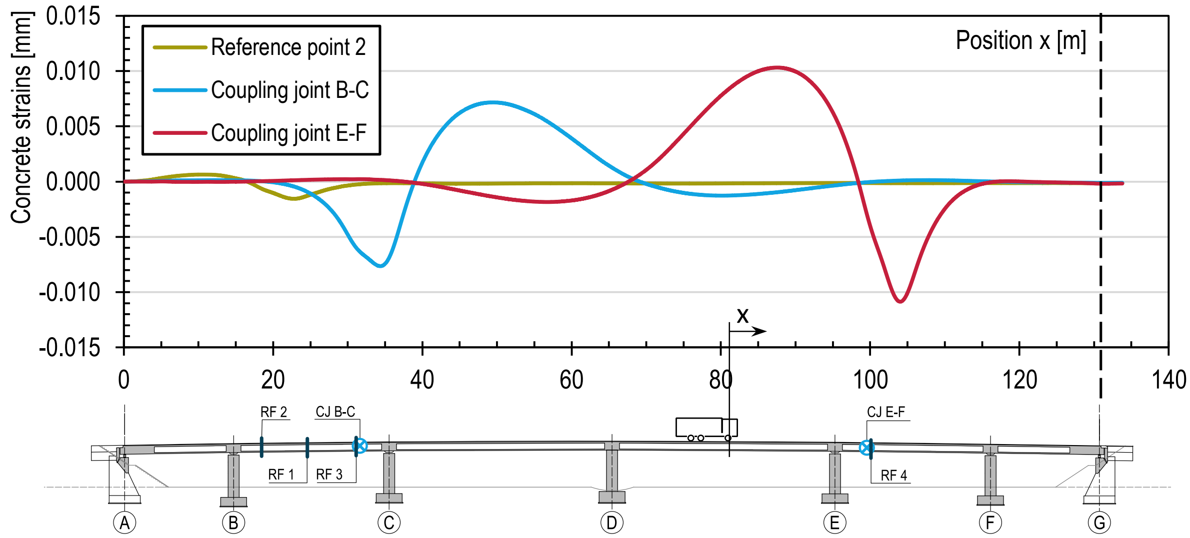


**Fig. 19** — Concrete strains in the coupling in reference point 2 vs the position of the trucks

This indicates the presence of cracks in both coupling joints, which was expected. Because the coupling joints are also construction joints, no tensile stresses can be transferred across the joint via the concrete. A numerical model containing the whole superstructure was created to recalculate the test. In this model the superstructure was defined as beam-elements. Using this numerical model calibrated with the measured data (using mainly the deflections but also the strain-measurements), conclusions were drawn about crack depths and the stresses occurring in the tendons.

## SUMMARY AND CONCLUDING REMARKS

This paper describes the current practice of load testing of existing and new built concrete bridges in Germany. Since 2000 a guideline is regulating loading tests, but this guideline is preferably applicated for load test of existing building structures. Despite the very good experiences in a very large number of load tests on building structures, load testing of bridges is still an exception. However time and opinions are changing since there are strong demands for extending the life time of existing concrete bridges. The German Guideline is a valuable basis for engineers to plan, execute and evaluate load tests, but no specific rules for load testing of bridges are yet defined. Therefor further research is necessary to define basic regulations for load tests of concrete bridges. The high value of load testing for the overall evaluation of the bearing characteristics of concrete bridges is demonstrated in the described examples.

## REFERENCES


[1] Schacht, G.; Bolle, G.; Marx, S.: Loading Tests of Existing Concrete Structures – Historical Development and Present Practise. 4th International fib Congress, Prague, June 1 – June 4 2011, DVD.

[2] Zimmermann, H.: Einsturz einer Straßenbrücke bei Salez in der Schweiz, Centralblatt der Bauverwaltung (1884), S. 548–549.

[3] Stamm: Brückeneinstürze und ihre Lehren, Mitteilungen aus dem Institut für Baustatik, ETH Zürich, Zürich, Verlag Leeman (1952).

[4] Waldner, A.: Das Eisenbahnunglück bei Mönchenstein, Schweizerische Bauzeitung, Vol.17, Nr. 25, 26 und Vol.18, Nr. 1, 2, 3 (1891).

[5] https://en.wikipedia.org/wiki/Sydney_Harbour_Bridge: checked: 05/17/2017

[6] www.pictureaustralia.org

[7] DIN 1045 – Beton und Stahlbetonbau, Bemessung und Ausführung (Ausgabe 01.1972)

[8] Schmidt, H., Opitz, H.: Experimentelle Erprobung von Stahlbetonbauwerken in situ, 13. Kongress des IVBH in Helsinki, 6.–10.6.1988.

[9] TGL 33407/04 – Nachweis der Trag- und Nutzungsfähigkeit aufgrund experimenteller Erprobung, Fachbereichsstandard, November 1986.

[10] Steffens, K.: Experimentelle Traglastermittlung an Bauwerken – Grundlagen, Technik, Anwendungen; Schriftenreihe des Fachbereiches Bauingenieurwesen der Hochschule Bremen (1988), Heft 1.

[11] DAfStb-Richtlinie Belastungsversuche an Betonbauwerken, Ausgabe September 2000, Beuth Verlag GmbH, Berlin und Köln.

[12] Schacht, G.; Bolle, G.; Marx, S.: Belastungsversuche – Internationaler Stand des Wissens. Bautechnik 93 (2016) 2, S.85-97. DOI: 10.1002/bate.201500097

[13] DIN EN 1992. Design of concrete structures. 2012

[14] Marx, S.; Bolle, G.; Schacht, G.: Kapitel 3.2 – Bestandsaufnahme und Bestandsbewertung und Kapitel 7 – Bewertung der Tragfähigkeit auf Grundlage von Belastungsversuchen. In: Fingerloos, F.; Schnell, J.; Marx, S. (Hrsg.): Tragwerksplanung im Bestand, Betonkalender 2015.

[15] Schacht, G.; Bolle, G.; Marx, S.: Load Testing of Concrete Structures in Germany – General practice and recent developments. fib symposium 2017, Maastricht, 12-14 Juni 2017.

[16] Schacht, G.; Bolle, G.; Curbach, M.; Marx, S.: Experimentelle Bewertung der Schubtragsicherheit von Stahlbetonbauteilen. Beton- und Stahlbetonbau 111 (2016) 6, S. 343-354. DOI:10.1002/best.201600006

[17] Steffens, K.; Gutermann, M.: Entwicklung, Bau und Erprobung eines Belastungsfahrzeuges. Abschlussbericht, Hochschule Bremen, 2002.

[18] Gutermann, M.; Schröder, C.: 10 Jahre Belastungsfahrzeug BELFA. Bautechnik, 88 (2011) p. 199–204. doi:10.1002/bate.201110020

[19] Bretschneider, N.; Fiedler, L.; Kapphahn, G.; Slowik, V.; Technische Möglichkeiten der Probebelastung von Massivbrücken. Bautechnik, 89 (2012) p.102–110. doi:10.1002/bate.201100010

[20] Richtlinie für die Nachrechnung von Straßenbrücken im Bestand. BMVI. 2011

[21] Lantsoght, E.; van der Ven, C.; de Boer, A.; Hordijk, D.: Proof load testing of reinforced concrete slab bridges in the Netherlands, Structural Concrete, 2017. https://doi.org/10.1002/suco.201600171

[22] Lantsoght, E.; Yang, Y.; van der Ven, C.; de Boer, A.; Hordijk, D.: Ruytenschildt Bridge: Field and laboratory testing. Engineering Structures 128 (2016), p. 111-123.

[23] Busch, E.; Ehmann, R.; Steffens, K.: Spannbetonbrücke Baiersdorf über den Main-Donau-Kanal - Hybride Standsicherheits- und Gebrauchstauglichkeitsbewertung. Bautechnik 72 (1995) 3, S. 152-162.

[24] Schacht, G.; Piehler, J.; Müller, J.Z.A.; Marx, S.: Belastungsversuche an der historischen Gewölbebrücke über die Aller bei Verden. Bautechnik 94 (2017) 2, S.125-130 DOI: 10.1002 / bate.201600084

[25] Schacht, G.; Schwinge, E.; Krontal, L.; Hahn, O.; Marx, S.: Die Allerbrücke in Verden. In Jäger, W. (Hrsg.): Mauerwerkskalender, Ernst & Sohn, 2018.

[26] Marx, S.; Herrmann, R.; Wenner, M.; Schenkel, M.; Curbach, M. (Hrsg.): Monitoring an Talbrücken im Eisenbahnhochgeschwindigkeitsverkehr, Tagungsband des 23. Dresdner Brückenbausymposiums. Planung, Bauausführung, Instandsetzung und Ertüchtigung von Brücken. Dresden, 12. März 2013. Technische Universität Dresden, S. 131-152.

[27] Marx, S.; Beltran, R.; Wenner, M.: Long-term behaviour of integral concrete constructions subjected to axial internal forces induced by constraint, Fischer. O.; (Hrsg.) Proceedings of the 10th Japanese - German Bridge Symposium, Munich, Germany 16.-19 September 2014

[28] Wenner, M.; Marx, S.: Concrete slab track - bridge interaction and its impact on bridge design, Avraham N. Dancygier (Hg.): Proceedings of the fib Symposium. Engineering a concrete future: Technology, Modeling & Construction. Tel Aviv, Israel, 22-24 April 2013, p. 403-406.

[29] Marx, S.; Wenner, M.: Structural Health Monitoring (SHM) an der Scherkondetalbrücke: eine semi-integrale Eisenbahn-Betonbrücke, Beton- und Stahlbetonbau Spezial (2015), p. 2-8, Ernst & Sohn, 2015

[30] Wenner, M.; Lippert, P.; Plica, S.; Marx, S.: Längskraftabtragung auf Eisenbahnbrücken Teil 1: Geschichtliche Entwicklung und Modellbildung. Bautechnik 93 (2016) 2, p. 59-67. DOI: 10.1002/bate.201500107

[31] Wenner, M.; Lippert, P.; Plica, S.; Marx, S.: Längskraftabtragung auf Eisenbahnbrücken Teil 2: Hintergründe des Nachweises, Bautechnik 93 (2016) 7, p. 470-481. DOI: 10.1002/bate.201600034

# DIAGNOSTIC LOAD TESTING OF CONCRETE BRIDGES, PRINCIPLES AND EXAMPLE

Joan Ramon Casas, Piotr Olaszek, Juliusz Ciesla, Krzysztof Germaniuk

**Synopsis:** The paper presents principles of diagnostic load tests of concrete bridges performed in Europe and one example of application from Poland. The common basis of the load testing techniques and methods were developed within the European Research Project ARCHES (Assessment and Rehabilitation of Central European Highway Infrastructure) and the main objectives and results of the project will be presented herein. Based on that, an example of application will follow.

The presented example of load tests is an evaluation of newly built reinforced concrete slab bridge. The bridge is a seven-span continuous structure with spans length of 14.05+18.03+15.31+15.63+18.97+18.60+14.34 m [553+ 710+603+615+747+732+567 in]. After construction, during cleaning the bottom surface of the structure many cracks were noticed in the tension zone. The process of bridge load testing was concentrated on the analysis of the cause of cracks appearing and estimation of the load carrying capacity of the bridge. The investigation range contained the following: tests of material properties, analytical calculations, visual examination of the bottom surface of the structure before, during and after load testing; measurements under test loading: deflection, selected cracks width and supports displacement. The final conclusions included the causes of crack appearing and recommendations for the future bridge service.

**Keywords:** diagnostic load testing, concrete bridges, cracks